Journal of Applied Mechanics and Technical Physics, Vol. 49, No. 3, pp. 391–399, 2008

NUMERICAL CALCULATIONS OF SUPERSONIC UNDEREXPANDED JETS IN A COCURRENT FLOW WITH THE USE OF PARABOLIZED NAVIER–STOKES EQUATIONS

A. P. Makasheva and A. Zh. Naimanova

UDC 532.526

Results of a numerical study of three-dimensional supersonic jets propagating in a cocurrent flow are described. Averaged parabolized Navier–Stokes equations are solved numerically on the basis of a developed scheme, which allows calculations in supersonic and subsonic flow regions to be performed in a single manner. A jet flow with a cocurrent flow Mach number $0.05 \leqslant \mathrm{M}_\infty \leqslant 7.00$ *is studied, and its effect on the structure of the mixing layer is demonstrated. The calculated results are compared with available experimental and numerical data.*

Key words: *underexpanded supersonic jet, cocurrent flow, Navier–Stokes equations.*

Introduction. There are many experimental and theoretical investigations dealing with the structure of supersonic jet flows and its dependence on the jet pressure ratio and initial values of the Mach number, and temperature [1–6]. In particular, propagation of a system of supersonic jets in cocurrent supersonic and hypersonic flows has been well studied. Jet flows with moderate Mach numbers are also of interest for practice. The effect of the Mach number of the cocurrent flow M_∞ and the jet pressure ratio $n = p_0/p_\infty$ (p_0 and p_∞ are the pressure in the jet and in the cocurrent flow, respectively) on the supersonic jet flow was studied experimentally in [4]. It was demonstrated that there are qualitative and quantitative differences in the structure of the initial part of underexpanded jets for $\mathrm{M}_\infty = 0$–2 and $\mathrm{M}_\infty > 2$. In addition, disappearance of the central (normal) shock at $\mathrm{M}_\infty > 2$ was observed; the characteristic length of the initial part of the jet (distance from the nozzle exit) and the diameters of the barrel and central shock waves were found.

The main problem in the numerical solution of these problems is the presence of oscillations caused not only by discontinuities in the initial data, but also by the fact that the original system of equations is a system of a hyperbolic–parabolic type in supersonic flows and a system of an elliptic type in subsonic flows. For the equations to remain of a hyperbolic–parabolic type, the problem has to be regularized. The research performed in [2, 3] has to be noted among theoretical papers. Ishii et al. [2] considered the flow structure with exhaustion of a sonic jet into a cocurrent flow; they showed that the presence of normal shock waves (Mach disks) depends on the jet pressure ratio. No Mach disks arise at moderate jet pressure ratios ($n = 1.5$–2.0), and there is only a system of shock waves (this result was not confirmed by experiments performed in [4]). Abdol-Hamid and Wilmoth [1] assumed that the shock-wave structure is mainly affected by large-scale vortices in the jet, though it is known that viscous processes do not dominate at the initial part of the jet.

The goal of the present activities was a numerical study of the shock-wave structure of supersonic jets exhausting into a supersonic (subsonic) flow.

Formulation of the Problem. We consider the exhaustion of a system of three-dimensional viscous supersonic turbulent jets from circular nozzles into a cocurrent flow (Fig. 1). The jets and the cocurrent flow propagate in the x direction, and the y and z axes are perpendicular to the flow. The jets are arranged symmetrically

Institute of Mathematics, Ministry of Education and Science of the Kazakhstan Republic, Almaty 050010, Kazakhstan; ked@math.kz. Translated from Prikladnaya Mekhanika i Tekhnicheskaya Fizika, Vol. 49, No. 3, pp. 54–63, May–June, 2008. Original article submitted November 15, 2005; revision submitted May 31, 2007.

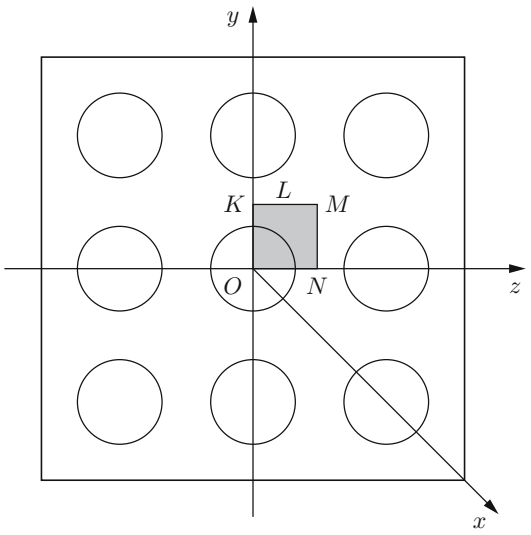

Fig. 1. Schematic pattern of the flow.

in both horizontal and vertical directions. As the system of jets is periodic, we consider a square with the side of length L bounded by the axes of symmetry of the jet and the flow. We find the solution of the problem in the hatched region $OKMN$ (Fig. 1), with the removed domain being replaced by the conditions of symmetry.

The original equations are the parabolized Navier–Stokes equations for the averaged flow, which are written in dimensionless form:

$$\frac{\partial \boldsymbol{E}}{\partial x} + \frac{\partial\,(\boldsymbol{F} - \boldsymbol{F}_v)}{\partial y} + \frac{\partial\,(\boldsymbol{G} - \boldsymbol{G}_v)}{\partial z} = 0. \tag{1}$$

In these equations,

$$\boldsymbol{E} = \begin{pmatrix} \rho u \\ \rho u^2 + p \\ \rho uv \\ \rho uw \\ (E_t + p)u \end{pmatrix}, \qquad \boldsymbol{F} = \begin{pmatrix} \rho v \\ \rho uv \\ \rho v^2 + p \\ \rho vw \\ (E_t + p)v \end{pmatrix}, \qquad \boldsymbol{G} = \begin{pmatrix} \rho w \\ \rho uw \\ \rho vw \\ \rho w^2 + p \\ (E_t + p)w \end{pmatrix},$$

$$\boldsymbol{F}_v = \frac{1}{\mathrm{Re}}\Big(0, \mu\,\frac{\partial u}{\partial y}, \frac{4}{3}\,\mu\,\frac{\partial v}{\partial y}, \mu\,\frac{\partial w}{\partial y}, u\mu\,\frac{\partial u}{\partial y} + \frac{4}{3}\,v\mu\,\frac{\partial v}{\partial y} + w\mu\,\frac{\partial w}{\partial y} + \frac{k}{(\gamma-1)\mathrm{M}_a^2\mathrm{Pr}}\,\frac{\partial T}{\partial y}\Big)^{\mathrm{t}},$$

$$\boldsymbol{G}_v = \frac{1}{\mathrm{Re}}\Big(0, \mu\,\frac{\partial u}{\partial z}, \mu\,\frac{\partial v}{\partial z}, \frac{4}{3}\,\mu\,\frac{\partial w}{\partial z}, u\mu\,\frac{\partial u}{\partial z} + v\mu\,\frac{\partial v}{\partial z} + \frac{4}{3}\,w\mu\,\frac{\partial w}{\partial z} + \frac{k}{(\gamma-1)\mathrm{M}_a^2\mathrm{Pr}}\,\frac{\partial T}{\partial z}\Big)^{\mathrm{t}},$$

where

$$p = (\gamma-1)\Big(E_t - \frac{1}{2}\,(\rho u^2 + \rho v^2 + \rho w^2)\Big), \qquad T = \frac{1}{\rho c_v}\Big(E_t - \frac{1}{2}\,(\rho u^2 + \rho v^2 + \rho w^2)\Big),$$

$$c_v = \frac{1}{\gamma(\gamma-1)\mathrm{M}_a^2}, \qquad \mu = \mu_l + \mu_t,$$

u, v, and w are the velocity components in the streamwise and crossflow directions, ρ is the density, p is the pressure, T is the temperature, E_t is the total energy, $\gamma = c_p/c_v$ is the ratio of specific heats, c_p and c_v are the specific heats at constant pressure and constant volume, respectively, M_a is the Mach number of the jet, Re is the Reynolds number, Pr is the Prandtl number, μ_t is the turbulent viscosity, and μ_l is the molecular viscosity calculated by Sutherland's formula $\mu_l = T^{3/2}(1 + S_1)/(T + S_1)$, where $S_1 = 110/T_0$.

The characteristics at the nozzle exit ρ_0, u_0, and T_0 are used as scale parameters, the reference scale for pressure and total energy is $\rho_0 u_0^2$, and the x, y, and z coordinates are normalized to the nozzle radius r_0. In what follows, the jet parameters and the flow parameters are indicated by the subscripts 0 and ∞, respectively.

In the calculations, we used two algebraic models of turbulence, which take into account the mixing length. In the initial part of exhaustion of a supersonic jet into a subsonic cocurrent flow and in the entire flow region in the case of streamwise injection of a supersonic jet into a supersonic cocurrent flow, the turbulent viscosity was calculated by the formula [7]

$$\mu_t = C\rho l(u_{\max} - u_{\min}), \tag{2}$$

where $l = (u_{\max} - u_{\min})/(|\partial u/\partial y|_{\max} + |\partial u/\partial z|_{\max})$ is the mixing length and C is an empirical coefficient.

The turbulent viscosity in the main part of the flow of a supersonic jet in a subsonic cocurrent flow was determined by the Baldwin–Lomax algebraic model of turbulence

$$\mu_t = I^k \rho l^2 |\Omega|,$$

where Ω is the vorticity and I^k is the limiter.

The initial and boundary conditions have the following form:

— for $x = 0$ in the jet,

$$u = 1, \qquad T = 1, \qquad \rho = 1, \qquad v = w = 0,$$

— for $x = 0$ in the flow,

$$T = 1, \qquad u = \frac{\mathrm{M}_a}{\mathrm{M}_\infty}\sqrt{T}, \qquad p = \frac{1}{\gamma n \mathrm{M}_a^2}, \qquad v = w = 0;$$

— for $x > 0$,

$$y = 0,\ y = L: \qquad v = 0, \qquad \frac{\partial u}{\partial y} = \frac{\partial w}{\partial y} = \frac{\partial p}{\partial y} = \frac{\partial T}{\partial y} = 0,$$

$$z = 0,\ z = L: \qquad w = 0, \qquad \frac{\partial u}{\partial z} = \frac{\partial v}{\partial z} = \frac{\partial p}{\partial z} = \frac{\partial T}{\partial z} = 0.$$

Method of the Solution. As the original equations include a streamwise pressure gradient, the disturbances can propagate upstream through subsonic regions of the flow field. For this reason, the marching method with respect to the spatial coordinate becomes ill-conditioned, which often leads to emergence of diverging solutions. There are several methods to eliminate potentially growing solutions. Similar to [8], the flow vector $\boldsymbol{E}$ is split in the present work into two components

$$\boldsymbol{E} = \boldsymbol{E}^* + \boldsymbol{E}^p, \qquad \boldsymbol{E}^* = \begin{pmatrix} \rho u \\ \rho u^2 + \omega p \\ \rho u v \\ \rho u w \\ (E_t + p)u \end{pmatrix}, \qquad \boldsymbol{E}^p = \begin{pmatrix} 0 \\ (1-\omega)p \\ 0 \\ 0 \\ 0 \end{pmatrix}. \tag{3}$$

According to Eqs. (3), there appears a parameter ω as a multiplier at the pressure gradient in the equation of motion along the streamwise coordinate x. An analysis of eigenvalues suggests that system (3) in a system of the hyperbolic–parabolic type in subsonic regions if $\omega \leqslant f(\mathrm{M}_x) = \sigma\gamma\mathrm{M}_x^2$ and in supersonic regions if $\omega = 1$ ($\mathrm{M}_x = u/c$ is the local Mach number).

With allowance for Eqs. (3), system (1) in the generalized coordinate system becomes

$$\frac{\partial \boldsymbol{E}^*}{\partial \xi} + \frac{\partial \boldsymbol{E}^p}{\partial \xi} + \frac{\partial (\boldsymbol{F} - \boldsymbol{F}_v)}{\partial \eta} + \frac{\partial (\boldsymbol{G} - \boldsymbol{G}_v)}{\partial \zeta} = 0, \tag{4}$$

where $\xi = \xi(x)$, $\eta = \eta(y)$, $\zeta = \zeta(z)$, $\boldsymbol{E} = J^{-1}\boldsymbol{E}$, $\boldsymbol{F} = \eta_y J^{-1}\boldsymbol{F}$, $\boldsymbol{G} = \zeta_z J^{-1}\boldsymbol{G}$, $\boldsymbol{F}_v = \eta_y J^{-1}\boldsymbol{F}_v$, $\boldsymbol{G}_v = \zeta_z J^{-1}\boldsymbol{G}_v$, and $J = \partial(\xi, \eta, \zeta)/\partial(x, y, z)$ is the Jacobian of transformation.

System (4) was solved by a shock-capturing marching method along the coordinate ξ with the use of a two-stage splitting scheme: flow transfer was assumed to be performed through convection at the first stage and through diffusion at the second stage.

Stage 1. Calculation of intermediate values of the flows:

$$\frac{\boldsymbol{E}^{*i} - \boldsymbol{E}^{*n}}{\Delta\xi} = -\frac{\partial \boldsymbol{F}^n}{\partial \eta} - \frac{\partial \boldsymbol{G}^n}{\partial \zeta} - \frac{\partial \boldsymbol{E}^p}{\partial \xi}. \tag{5}$$

Stage 2. Calculation of the final values of the sought quantities:

$$\frac{A^n(\boldsymbol{U}^{n+1}-\boldsymbol{U}^{*i})}{\Delta\xi}=\frac{\partial \boldsymbol{F}_v^{n+1}}{\partial\eta}+\frac{\partial \boldsymbol{G}_v^{n+1}}{\partial\zeta} \tag{6}$$

($\boldsymbol{U}=[\rho,\rho u,\rho v,\rho w,E_t]^{\mathrm{t}}$ and $A=\partial\boldsymbol{E}^*/\partial\boldsymbol{U}$ is the Jacobi matrix [8]).

The numerical solution of Eq. (5) for the flow $\boldsymbol{E}^{*i}$ was obtained by the explicit MacCormack scheme [8] ($i=2$) with the second order of accuracy in terms of spatial coordinates or by the three-step Warming–Kutler–Lomax scheme [8] ($i=3$) with the third order of accuracy. After calculating $\boldsymbol{E}^{*i}$, we determine the components of the vector $\boldsymbol{U}^{*i}$ from the first equation in system (3) (for simplicity, the superscript is further omitted). For this purpose, we have to solve two systems, each consisting of five nonlinear algebraic equations for supersonic and subsonic regions. For the supersonic region, the system of equations has the form

$$\begin{pmatrix} U_2 \\ U_2^2/U_1+(U_5-(U_2^2+U_3^2+U_4^2)/(2U_1))(\gamma-1) \\ U_2U_3/U_1 \\ U_2U_4/U_1 \\ [U_5+(\gamma-1)(U_5-(U_2^2+U_3^2+U_4^2)/(2U_1))]U_2/U_1 \end{pmatrix}=\boldsymbol{E}^{*i},\qquad \boldsymbol{E}^{*i}=\begin{pmatrix} E_1 \\ E_2 \\ E_3 \\ E_4 \\ E_5 \end{pmatrix}. \tag{7}$$

The solution of system (7) with respect to the vector $\boldsymbol{U}$ is written as

$$U_1=\frac{\gamma E_2E_1^2-E_1^2\sqrt{(\gamma E_2)^2-(\gamma^2-1)(2E_1E_5-E_3^2-E_4^2)}}{(\gamma-1)(2E_5E_1-E_3^2-E_4^2)},$$

$$U_2=E_1,\qquad U_3=\frac{E_3U_1}{E_1},\qquad U_4=\frac{E_4U_1}{E_1},\qquad U_5=\frac{1}{U_1}\Big(\frac{E_5U_1^2}{E_1}-(E_2U_1-E_1^2)\Big).$$

Here the discriminant equals zero at $\mathrm{M}_x=1$.

In determining the components of the vector $\boldsymbol{U}$ in the subsonic region of the flow, the sought system of equations is written in the form

$$\begin{pmatrix} U_2 \\ (U_2^2+\sigma E_1^2)/U_1 \\ U_2U_3/U_1 \\ U_2U_4/U_1 \\ [U_5+(\gamma-1)(U_5-(U_2^2+U_3^2+U_4^2)/(2U_1))]U_2/U_1 \end{pmatrix}=E^{*i},\qquad \mathrm{M}_x=\frac{E_1}{\sqrt{\gamma p\rho}}.$$

The solution of this system has the form

$$U_1=\frac{E_1^2}{E_2}(1+\sigma),\qquad U_2=E_1,\qquad U_3=\frac{E_3E_1^2}{E_1E_2}(1+\sigma),\qquad U_4=\frac{E_4E_1^2}{E_1E_2}(1+\sigma),$$

$$U_5=\Big(\frac{E_5E_1(1+\sigma)}{E_2}+\frac{\gamma-1}{2(1+\sigma)}\,\frac{E_2^2+E_3^2(1+\sigma)^2+E_4^2(1+\sigma)^2}{E_2}\Big)\frac{1}{\gamma}.$$

At the second stage, system (6) is solved by the three-step matrix sweep method.

At the last stage, the flow vector $\boldsymbol{U}$ in the vicinity of shock waves is explicitly smoothed to suppress solution oscillations, similar to [9]. The smoothing term is proportional to $(\Delta\eta)^4|p_{\eta\eta}|\boldsymbol{U}_{\eta\eta}$ and $(\Delta\zeta)^4|p_{\zeta\zeta}|U_{\zeta\zeta}$; its effect is most significant in flow regions with high pressure gradients. As is [9], the smoothing coefficient was varied in the range from 0 to 0.03.

Calculation Results. The parameters of coordinate transformation have the form [8]

$$\xi=x,\qquad \eta=B_y+\frac{1}{\tau}\operatorname{arsinh}\Big[\Big(\frac{y}{y'}-1\Big)\sinh(\tau B_y)\Big],$$

where

$$B_y=\frac{1}{2\tau}\ln\Big(\frac{1+(\mathrm{e}^{\tau}-1)(y'/L)}{1+(\mathrm{e}^{-\tau}-1)(y'/L)}\Big),$$

$0 < \tau < \infty$ is the extension parameter, and y' is the point with respect to which the grid is condensed. The transformation for $\zeta = \zeta(z)$ is similar to $\eta = \eta(y)$. To conserve the exact values on the jet boundary, the internal points in the vicinity of this boundary are redefined, similar to [10], by bilinear (if there is only one sought internal point) or linear (two points) interpolation. The calculations were performed in a domain with the transverse size of 7.5×7.5 on 100×100 and 200×200 grids. The step along the marching coordinate was varied in the range $\Delta\xi = 0.0006$–0.0015, and the transformation parameters were $\tau = 0.1$, $y' = 1$, and $z' = 1$. The coefficient $C = 0.05$ in Eq. (2) was chosen on the basis of test calculations. The numerical study was performed with the following values of the characteristic parameters: $\gamma = 1.4$, $1 \leqslant \mathrm{M}_a \leqslant 3$, $0.05 \leqslant \mathrm{M}_\infty \leqslant 7.00$, $1 \leqslant n \leqslant 10$, and $\mathrm{Re} = 10^4$. System (5) was solved by the two-step MacCormack method.

The calculation method proposed was tested by the problem of exhaustion of a system of plane supersonic jets of an ideal gas into a cocurrent supersonic flow with the parameters $\mathrm{M}_a = 3$, $\mathrm{M}_\infty = 5$, $n = 10$, and $T_0 = T_\infty = 1$, and by the problem of exhaustion of a turbulent axisymmetric supersonic jet into a subsonic cocurrent flow ($\mathrm{M}_a = 3$, $\mathrm{M}_\infty = 0.05$, $n = 1$, and $T_0 = T_\infty = 1$). Hereinafter, the method of global iterations was additionally used if the problems considered had vast subsonic regions. The initial approximation of the pressure distribution in the entire flow region was defined. Then, the initial equations were solved for the known pressure field by the marching algorithm (5). The pressure used for the next iteration was preserved at each step. The calculations were continued until a necessary accuracy of approximation was reached, i.e., until the change in pressure between the neighboring iterations became insignificant:

$$|p^{n+1,k+1} - p^{n+1,k}| < \delta_p \ll 1$$

($\delta_p = 10^{-4}$).

The calculated results are in good agreement with the experimental data [11], and only two global iterations were needed.

The spatial structure of a system of underexpanded supersonic jets exhausting into a supersonic cocurrent flow is shown in Fig. 2. As the jet propagates downstream (from the initial region into the cocurrent flow with a lower pressure), a shock wave starts propagating, which then becomes reflected from the centerline. As the Mach number of the cocurrent flow increases, the velocity of shock-wave propagation decreases: in the cross section $x = 28.7$, the shock wave reaches the centerline at $\mathrm{M}_\infty = 7$ (right picture in Fig. 2d), whereas it experiences a secondary reflection from the jet centerline at $\mathrm{M}_\infty = 2$ (left picture in Fig. 2d). As a consequence, different spatial patterns of the flow arise, caused by interaction of waves reflected from the y and z axes (cf. left picture in Fig. 2d and right picture in Fig. 2e).

The analysis of the fields of the Mach contours of streamwise velocities suggests that the jet boundary has a barrel shape at $\mathrm{M}_\infty = 2$ (see left pictures in Figs. 2f and 2g), whereas the jet width increases along the x axis almost linearly with increasing distance from the nozzle exit at $\mathrm{M}_\infty = 7$ (see right pictures in Figs. 2f and 2g).

It is known that the barrel shape of the jet boundary is typical of supersonic jets exhausting into a subsonic cocurrent flow. Therefore, we calculated the exhaustion of a single supersonic turbulent circular jet into a subsonic cocurrent flow with the parameters $\mathrm{M}_a = 2$, $\mathrm{M}_\infty = 0.05$–0.25, $n = 1.45$, and $T_0 = T_\infty = 1$. The pressure distribution in the plane xy (Fig. 3a) shows that a bunch of expansion waves arise near the nozzle edge because of the difference in pressure in the jet and the cocurrent flow. In passing through these expansion waves, the pressure decreases, and the pressure in the greatest cross section of the jet becomes lower than the ambient pressure. The streamline become deflected from the jet centerline, i.e., the jet becomes expanded (Fig. 3b). Then the expansion waves reach the jet boundary and become reflected from it in the form of compression waves; as a result, the pressure in the jet increases. In what follows, as is shown in Fig. 3a, the spectrum of the wave is repeated, and the jet boundary ($\mathrm{M} = 0.25$) acquires a wavy (barrel) shape.

Apparently, the barrel shape of the jet boundary for $\mathrm{M}_\infty \leqslant 2$ (see left picture in Fig. 2) is caused by the fact that the intensity of waves reflected from the jet boundary is of the same order as the intensity of waves reflected from the domain under consideration.

Figure 3c shows the pressure distribution on the jet centerline, which is compared with the calculated and experimental data of [1]. It should be noted that the code developed in [1] allows calculations for $\mathrm{M}_\infty = 0.25$; therefore, the results of the present work and of [1] are compared at $\mathrm{M}_\infty = 0.25$. The results in Fig. 3c are in good agreement as a whole, through there appears some difference between the calculations performed in the present work and the experimental data, as the distance from the nozzle increases.

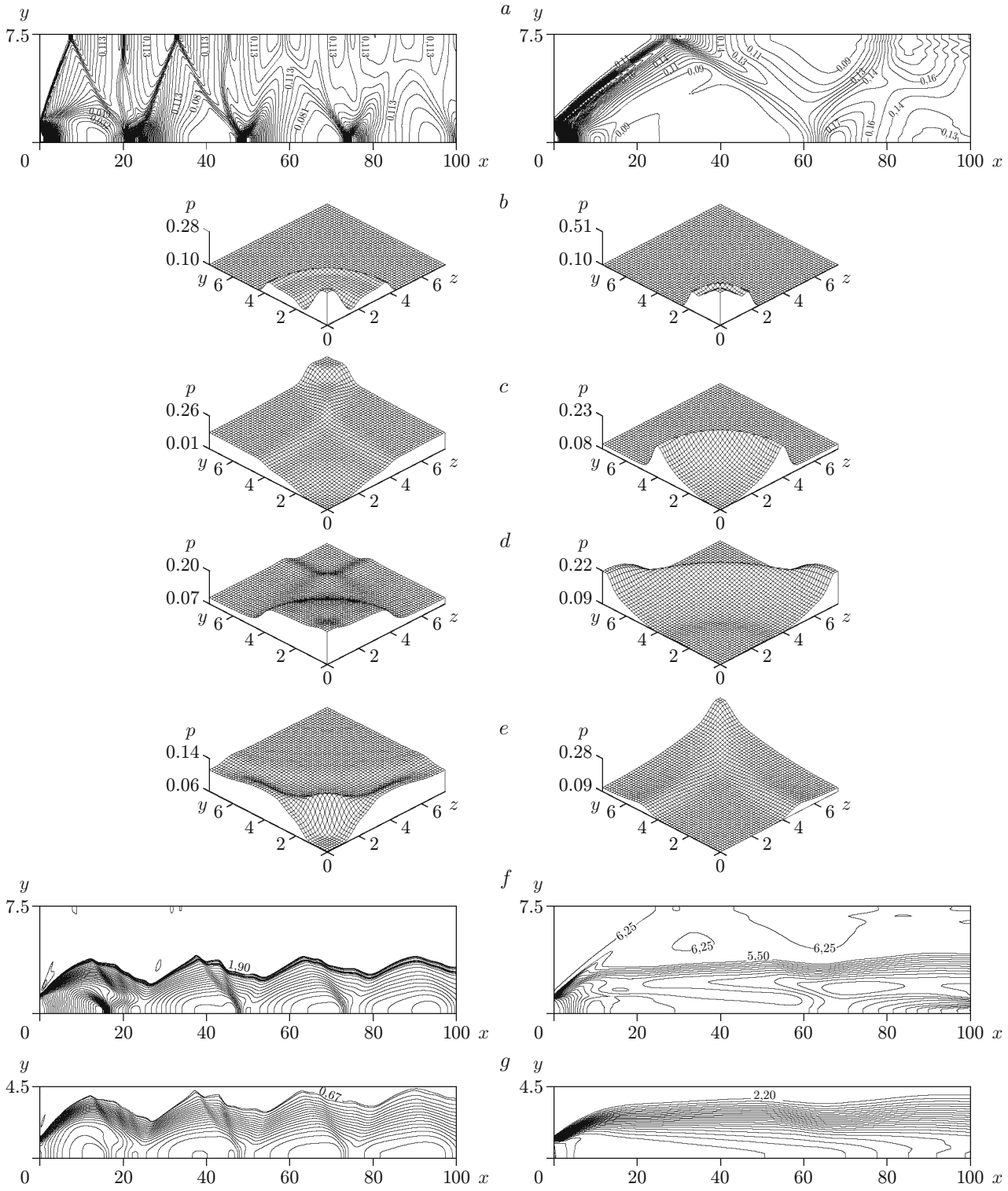

Fig. 2. Distributions of gas-dynamic parameters ($M_a = 3$, $n = 10$, and $T_0 = T_\infty = 1$) for $M_\infty = 2$ (left pictures) and $M_\infty = 7$ (right pictures); (a) isobars; (b–e) pressure profiles in the cross sections $x = 3.2$ (b), 12.7 (c), 28.7 (d), and 44.6 (e); (f) Mach contours with a step of 0.15; (g) isolines of the streamwise velocity with a step of 0.05.

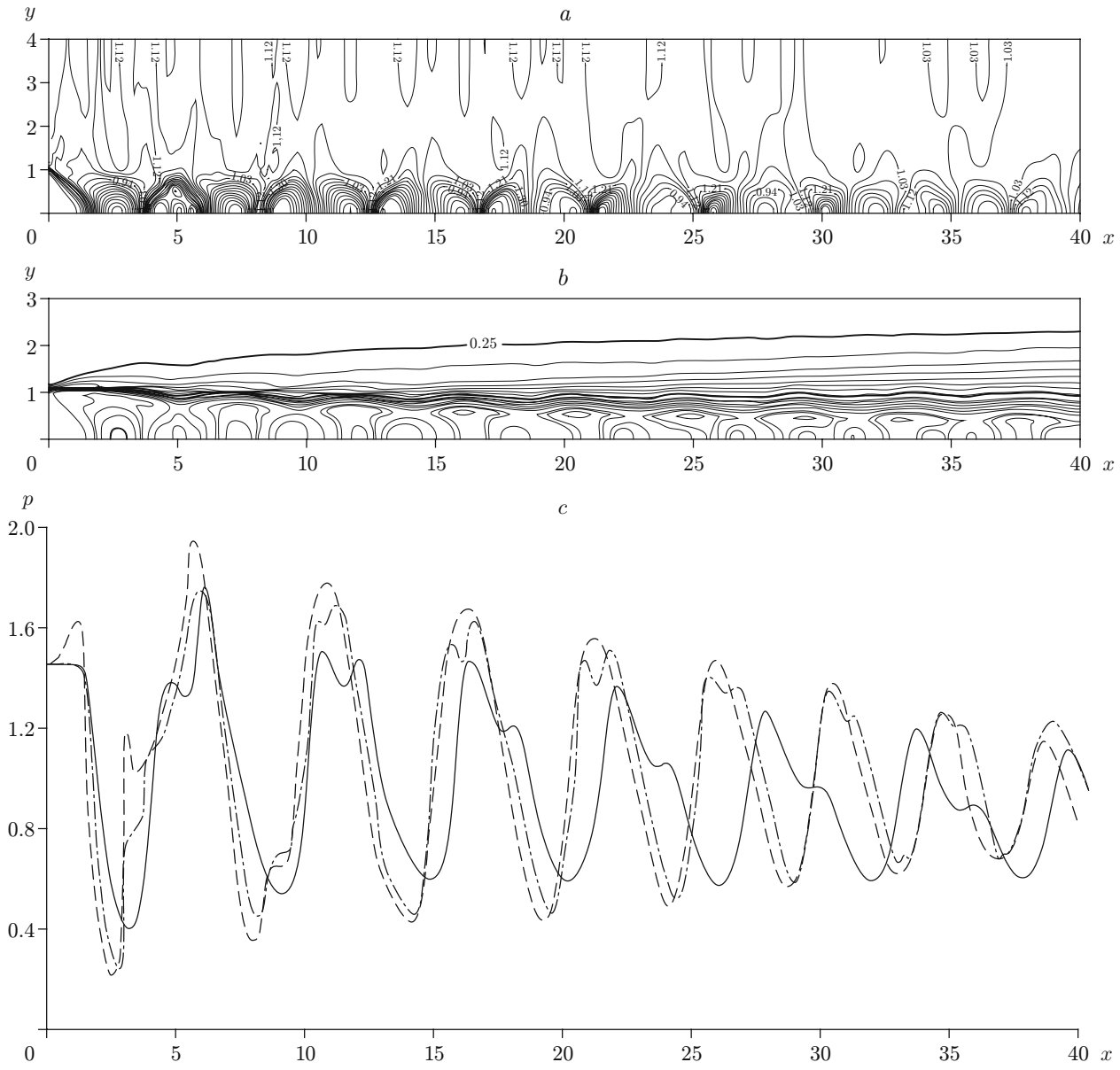

Fig. 3. Isobars (a), Mach contours with a step of 0.05 (b), and pressure distribution along the x axis (c) for $M_a = 2$, $M_\infty = 0.25$, $n = 1.45$, and $T_0 = T_\infty = 1$: the solid curves are the results obtained in the present work; the dashed curves are the experimental data of [1]; the dot-and-dashed curves are the results calculated in [1].

The effect of the Mach number M_∞ on the flow characteristics is illustrated in Fig. 4. In the initial part (in the region of the first "barrel" at $x \approx 6$), the transverse size of the jet is identical for all values of M_∞. In the main part, the greatest expansion of the jet is observed for $M_\infty = 0.05$ (Fig. 4a). This result is validated by the experiment [4], which showed that the length of the initial part of an underexpanded jet exhausting into a subsonic cocurrent flow depends weakly on the value of M_∞. It follows from Fig. 4b that the difference in the pressure distributions becomes more pronounced (except for the first phase) with increasing Mach number of the cocurrent flow.

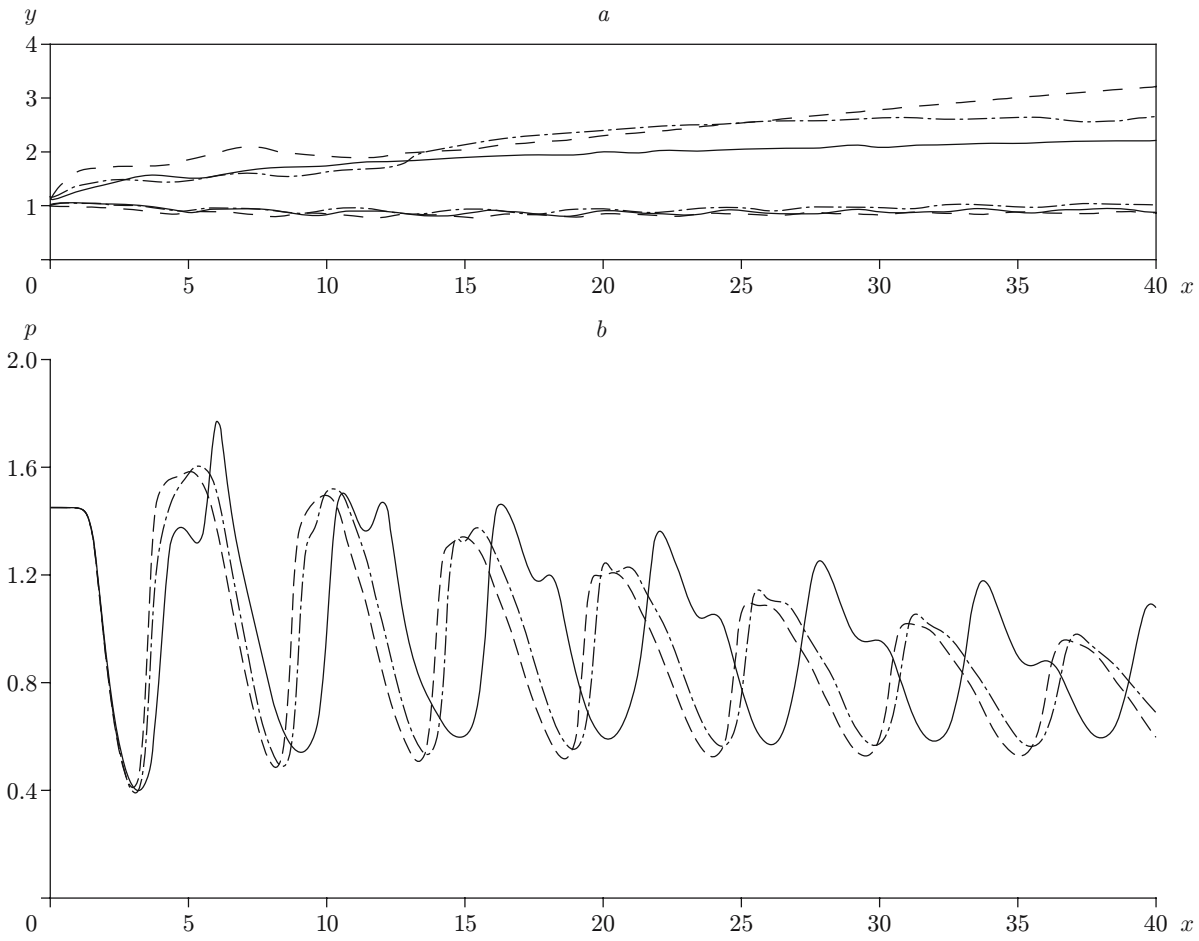

Fig. 4. Mach contours (a) and pressure distribution along the x axis (b) for $M_a = 2$, $n = 1.45$, and $T_0 = T_\infty = 1$: $M_\infty = 0.25$ (solid curves), 0.1 (dot-and-dashed curves), and 0.05 (dashed curves).

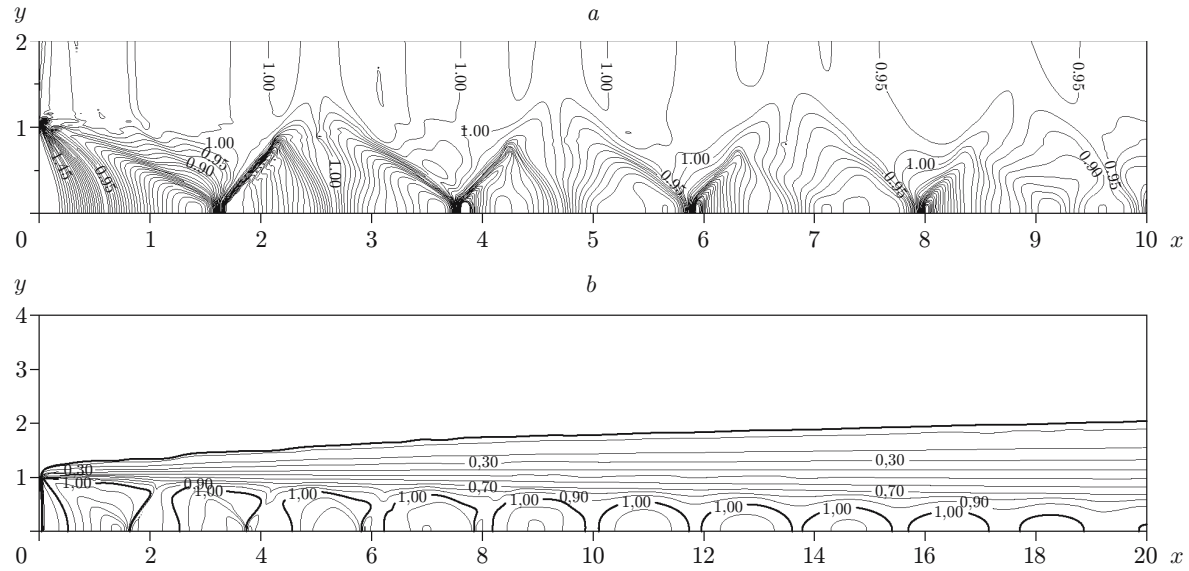

Fig. 5. Isobars (a) and Mach contours (b) in the plane xy for $M_a = 1.02$, $M_\infty = 0.05$, $n = 1.62$, and $T_0 = T_\infty = 1$.

It follows from the results calculated for a sonic jet ($M_a = 1.02$, $M_\infty = 0.05$, $n = 1.62$, and $T_0 = T_\infty = 1$) that barrel shock waves are formed in the flow (Fig. 5a), which are classified as the central and the reflected shock wave. The pressure behind the reflected shock wave and also behind the central shock wave is higher than the ambient pressure, and the flow is again accelerated. It follows from Fig. 5b that a weak normal shock wave (Mach disk) is formed in the flow. The flow at the periphery, behind the reflected shock wave, can be either completely supersonic or partly subsonic. For instance, as it follows from numerical experiments, the flow is subsonic in the first four barrels, the flow behind the fifth barrel is supersonic, and the region of the supersonic flow is located inside the region of the subsonic flow at $x < 12$.

Thus, the exhaustion of a system of supersonic jets into a supersonic cocurrent flow and the exhaustion of a single supersonic jet into a subsonic cocurrent flow are studied with the use of the numerical model constructed; the effect of the Mach number of the cocurrent flow on the shock-wave structure is considered; the jet boundary is demonstrated to have a barrel shape in the range $0.05 \leqslant M_\infty \leqslant 2.00$; a series of barrel shock waves is found to form in the case of exhaustion of a sonic jet from the nozzle; the calculated results are found to be in good agreement with available numerical and experimental data.

REFERENCES

1. K. S. Abdol-Hamid and R. G. Wilmoth, "Multiscale turbulence effects in underexpanded supersonic jets," *AIAA J.*, **27**, No. 3, 315–322 (1989).
2. R. Ishii and Y. Umeda, "Numerical analysis of two-phase jets," *J. Thermophys. Heat Transfer*, No. 1, 17–24 (1988).
3. E. Rathakrishnan, "A numerical approach to single and twin supersonic jet flows," in: www.ieindia.org /publish/as/1103/nov03as2.pdf.
4. V. S. Avduevskii, A. V. Ivanov, I. M. Karpman, et al., "Structure of turbulent underexpanded jets exhausting into the ambient space and cocurrent flow," *Izv. Akad. Nauk SSSR, Mekh. Zhidk. Gaza*, No. 3, 15–29 (1972).
5. A. Mohamed, A. Hamed, and T. Lehnig, "Supersonic rectangular over-expanded jets of single and two-phase flows," in: www.fluent.com/solutions/aerospace/pdfs/ex.228.pdf.
6. V. I. Zapryagaev, N. P. Kiselev, and A. A. Pavlov, "Effect of streamline curvature on intensity of streamwise vortices in the mixing layer of supersonic jets," *J. Appl. Mech. Tech. Phys.*, **45**, No. 3, 335–434 (2004).
7. V. N. Vatsa, M. J. Werle, O. L. Anderson, and G. B. Hankins (Jr.), "Solutions for three-dimensional over- or underexpanded exhaust plumes," *AIAA J.*, **20**, No. 9, 1188–1194 (1982).
8. D. Anderson, J. Tannehill, and R. Pletcher, *Computational Fluid Mechanics and Heat Transfer*, Hemisphere, New York (1984).
9. N. D. Sinha and S. M. Dash, "Parabolized Navier–Stokes analysis of ducted supersonic combustion problems," J. Propuls. Power, No. 5, 455-464 (1987).
10. Jungwoo Kim, Dongjoo Kim, and Haecheon Choi, "An immersed-boundary finite-volume method for simulations of flow in complex geometries," *J. Comput. Phys.*, No. 171, 132–150 (2001).
11. G. N. Abramovich, *Theory of Turbulent Jets* [in Russian], Nauka, Moscow (1984).